JOURNAL OF GEOPHYSICAL RESEARCH, VOL. 103, NO. C3, PAGES 5419–5428, MARCH 15, 1998

Path of the North Atlantic Deep Water in the Brazil Basin

Norbert Zangenberg and Gerold Siedler
Institut für Meereskunde, Kiel, Germany

Abstract. Recent hydrographic sections and high-quality historical data sets are used to determine geostrophic currents at subtropical latitudes in the western basin of the South Atlantic. Levels of no motion are determined from water mass information and a mass balance constraint to obtain the transport field of North Atlantic Deep Water (NADW) in this region. The incoming NADW transport of about 20 Sv from the north at 19°S appears to be balanced by only one third of this transport leaving in the south and two thirds leaving to the east or northeast at the Mid-Atlantic Ridge. A simple model is proposed to determine the cause of the NADW branching. It is shown that potential vorticity preservation in the presence of topographic changes leads to a similar flow pattern as observed, with branching near the Vitória-Trindade-Ridge and also an eastward turning of the southward western boundary current at about 28°S, the latitude where a balance of planetary vorticity change and stretching can be expected.

1. Introduction

Observations of the structure, the path, and the transport rates of the North Atlantic Deep Water (NADW) have played an important role in developing the dynamical framework of deep western boundary currents and the global thermohaline circulation [e.g., *Warren*, 1981; *Broecker*, 1991]. The pioneering work of *Stommel* [1958], *Stommel et al.* [1958], and *Stommel and Arons* [1960] provided the basic understanding of global flow patterns, with western boundary currents feeding the broad interior poleward flow (Figure 1). Their models with simple geometry and without stratification cannot be expected to provide any details of the flow. Nevertheless, the large-scale transport pattern in the South Atlantic from such a model, however crude, still seems to outline the basic pattern of NADW spreading in this part of the global ocean.

Observations of a southward deep water flow between intermediate and bottom water in the western South Atlantic date back to the works of *Brennecke* [1911] and *Wüst* [1935], who described three layers of the NADW related to different sources and showed a dominance of southward NADW transport in the western South Atlantic. The distribution of oxygen given by *Wüst and Defant* [1936, Figure XVIII] in the middle NADW, characterized by an oxygen maximum, indicated three tongues, suggesting a spreading southward along the South American continental slope, eastward close to the equator, and eastward from the Brazil Basin.

Observations in the South Atlantic in recent years have provided a much extended hydrographic database facilitating a closer look at the structure and transports of NADW [*McCartney*, 1993; *De Madron and Weatherly*, 1994; *Rhein et al.*, 1995; *Siedler et al.*, 1996]. The presentation of salinity at 3000 m in Figure 2, adapted from *Gouretski and Jancke* [1995], suggests the three branches of NADW. *Tsuchiya et al.* [1994] presented an oxygen map with a similar pattern. The zonal flow component at tropical latitudes was studied by *Friedrichs et al.* [1994], who found an eastward flow of 7 Sv (1 Sv = 10^6 m^3 s^{-1}) of lower NADW which seems to spread into the eastern basin in the area of the Romanche Fracture Zone. *De Madron and Weatherly* [1994] described a major reduction of the net southward NADW transports from 24 Sv to 7 Sv between 18°S and 24°S. *Zemba* [1991] investigated the water mass distributions at higher latitudes in the western South Atlantic and estimated a poleward flow of 10 Sv of NADW within the deep western boundary current at 27°S.

The area of this study is presented in Figure 3. Prominent features in the Southern Brazil Basin region are the Mid-Atlantic Ridge in the east, the ridge from the Santos Plateau across the Rio Grande Rise to the Mid-Atlantic Ridge in the south and the seamount and island chain of the Vitória-Trindade Ridge. They all provide topographic obstacles to the deep water flow.

Paper number 97JC03287.
0148-0227/98/97JC-03287$09.00

2. Data

The main source of data from the Brazil Basin used here are hydrographic sections occupied by the research vessel *Meteor* during 1990/1991 (cruise 15 [*Siedler and Zenk*, 1992]) and 1992/1993 (cruise 22 [*Siedler et al.*, 1993]) as part of the World Ocean Circulation Experiment (WOCE) South Atlantic program. Lines A–D in Figure 4 denote the sections made in 1990/1991. The western end of D was repeated in 1992/1993. The section along 19°S has the WOCE designation A9, and that along 30°S is A10. Station separations were usually close to or smaller than the first internal local Rossby radius (40–60 km [*Houry et al.*, 1987]), and station spacing was further reduced in areas of steep bottom topography. Supplementing these two sets of *Meteor* data are observations made from Knorr and Melville in 1988/1989 as part of the South Atlantic Ventilation Experiment (SAVE) and from Oceanus cruise 133 in 1983. Their locations are shown in Figure 4, while the complete hydrographic data set used here is summarized in Table 1.

3. Method for Determining Geostrophic Transports

We will use the traditional approach of choosing a level of no motion in accordance with water mass properties. Diapycnal mixing between the defined water masses will be neglected

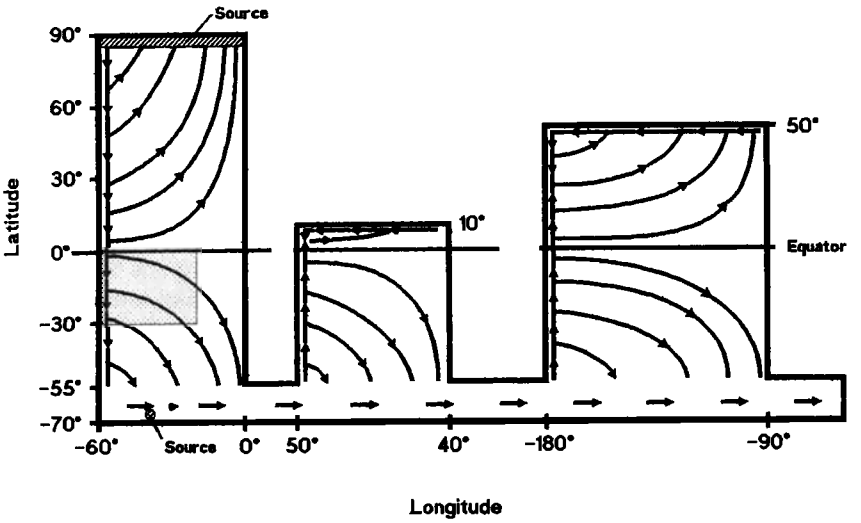

Figure 1. Global flow pattern of the deep ocean obtained from the Stommel-Arons circulation model [adapted from *Kuo and Veronis*, 1973]. The area investigated in the present study is shaded.

in the limited region of investigation. Additional constraints will be used, however. Minimizing the net balance in a box comprising most of the region will be required, and a check will be made on transport changes in the case of transition from one level of no motion to another.

First, we need to define the water mass boundaries. *Reid* [1989] and *Rintoul* [1991] obtained similar circulation patterns in the region of our study both for the Antarctic Intermediate Water and the Upper Circumpolar Deep Water. For transport calculations they are therefore combined here as Antarctic Intermediate Water (AAIW). The Weddell Sea Deep Water only extends to the northern part of the Argentine Basin as a substantial water mass [*Peterson and Whitworth*, 1989], and its contribution to the Southern Brazil Basin is an integral part of the bottom water flow. For the determination of near-bottom transports in the Southern Brazil Basin the sum of the water originating from the Weddell Sea and the circumpolar region will therefore be summarized as Antarctic Bottom Water (AABW). The classification of water masses by density surfaces is listed in Table 2. Corresponding salinity and density sections at 19°S and 30°S are shown in Figures 5a to 5d. More details on these sections are given by *Siedler et al.* [1996].

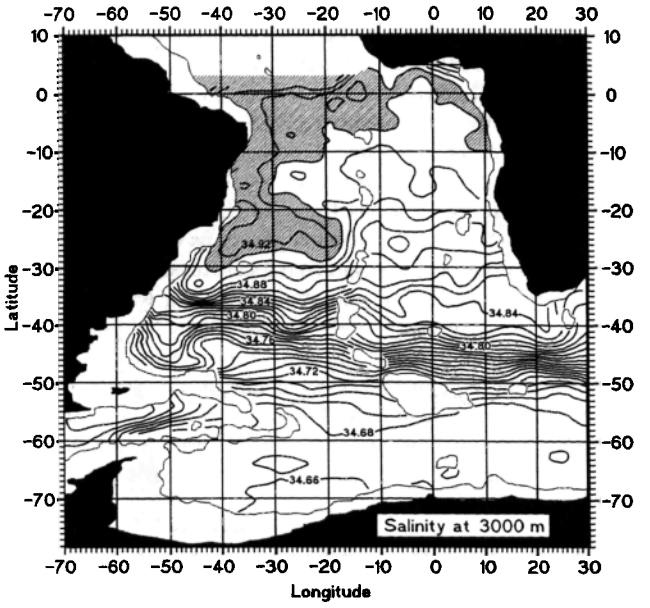

Figure 2. Horizontal salinity distribution at 3000 m derived from observations in the South Atlantic [after *Gouretski and Jancke*, 1995].

Appropriate levels of no motion can be expected at the boundaries of water masses which have opposite spreading directions. The AABW crosses the Rio Grande Ridge along the slope of the Santos Plateau and through the Vema and Hunter Channels [*Hogg et al.*, 1982; *Speer and Zenk*, 1993; *Pätzold et al.*, 1996] to the north. However, the NADW will have a southward component in the deep western boundary current. In the Southern Brazil Basin the interface between NADW and AABW can therfore be expected to represent a level of no motion. We use the isopycnal surface $\sigma_4 = 45.87$ kg m^{-3} as interface (Figures 5c and 5d) which closely corresponds to the 2°C isotherm of potential temperature [*Broecker et al.*, 1976; *De Madron and Weatherly*, 1994]. At the upper part of the continental slope, however, owing to the absence of AABW this isopycnal surface is not available.

Long-term current measurements on the continental slope at 23°S and 28°S [*Müller et al.*, this issue] show poleward flow components throughout the whole water column at this depth range, with speeds decreasing toward the bottom. For this reason we will take the bottom as level of no motion there.

Farther away from the Rio Grande Ridge in the Brazil Basin, the AABW flow probably has reversals in direction [*Speer and Zenk*, 1993; *De Madron and Weatherly*, 1994], and the AABW/NADW interface may therefore no longer be a level of strong directional change. In this part of the Brazil Basin the AAIW/NADW interface, however, will provide a good choice for the level of no motion. While the AAIW has westward and southward flow components near the Rio Grande Ridge [*Boebel et al.*, 1997], a northward or eastward spreading of AAIW can be expected farther north [*Reid et al.*, 1977; *Gordon and Greengrove*, 1986; *Ollitrault et al.*, 1995]. As a consequence, the AAIW and NADW will have opposing current directions in that northern region. We select the iso-

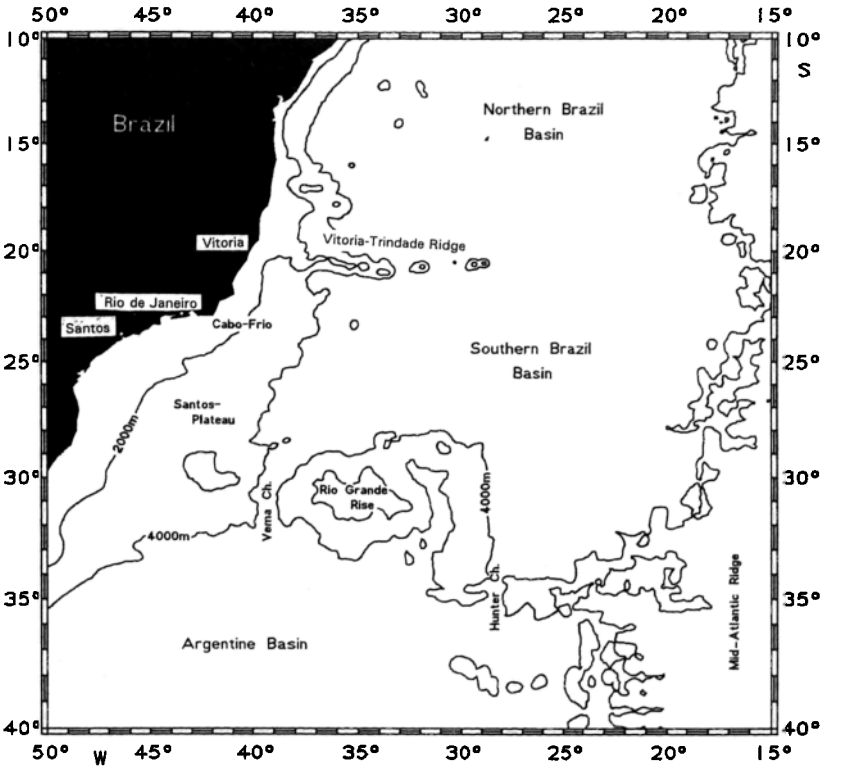

Figure 3. Map of the Southern Brazil Basin.

pycnal surface σ_2 = 36.70 kg m^{-3} (Figures 5c and 5d) to identify this interface. The near-bottom transport between neighboring stations with different bottom depths is estimated following the procedure described by *McCartney and Curry* [1993]. The shear between station pairs above the greatest common depth is extrapolated downward applying weights dependent on the vertical density gradient. The total contribution of the bottom triangles to the transports varies from about 3% for section WOCE A9 to about 6% in sections C and D. Even when assuming a poor approximation by the above method, the resulting errors will be within a few percent.

It was assumed that diapycnal processes do not contribute significantly to the transports, and water mass layers can be considered separately in this case. The transports in each water

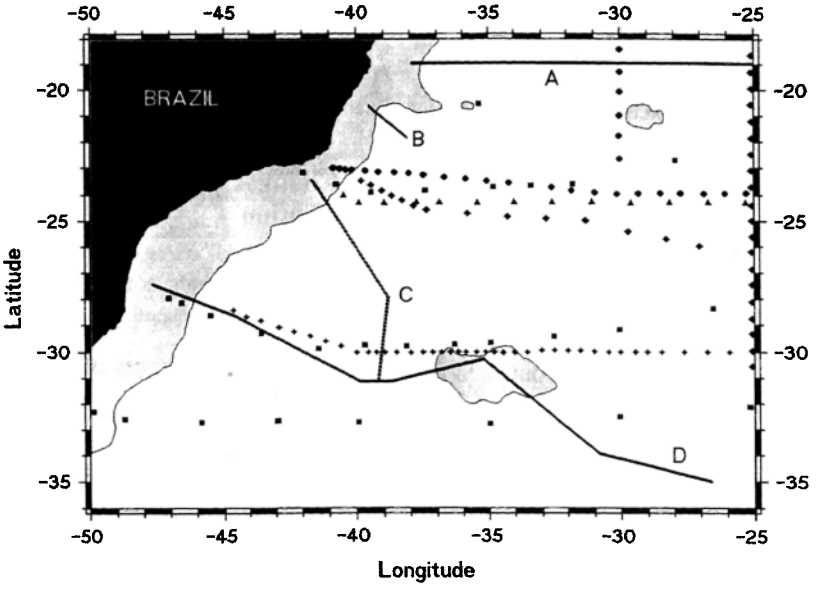

Figure 4. Distribution of the observational data used in this study. A–D indicate *Meteor* cruise 15 (1991); plus signs indicate *Meteor* cruise 22 (1992/1993); circles indicate *Oceanus* cruise 133 (1983); diamonds indicate SAVE/*Knorr* and *Melville* cruises (1988/1989); triangles indicate International Geophysical Year *Crawford* cruise (1958); and squares indicate *Meteor* cruise (1925–7).

Table 1. Observational Data Sets Used in the Present Study

Data Set	Location	Sampling Date	Reference
Crawford	24°S	1958	*Fuglister* [1960]
Meteor 1925–1927	24°S	1925–1927	*Wüst* [1935]
Meteor 1925–1927	28°S	1925–1927	*Wüst* [1935]
Meteor 1925–1927	32°S	1925–1927	*Wüst* [1935]
Meteor cruise 15	19°S	Feb.–March 1991	*Siedler and Zenk* [1992]
Meteor cruise 15	21°S	Feb. 1991	*Siedler and Zenk* [1992]
Meteor cruise 15	30°S	Jan. 1991	*Siedler and Zenk* [1992]
Meteor cruise 15	40°W	Jan. 1991	*Siedler and Zenk* [1992]
Meteor cruise 22	28°S	Nov.–Dec. 1992	*Siedler et al.* [1993]
Meteor cruise 22	30°S	Jan. 1993	*Siedler et al.* [1993]
Oceanus cruise 133	23°S	Feb. 1983	*Warren and Speer* [1991]
Knorr, SAVE Leg 3	23°S	Feb. 1988	SIO* (1992)
Melville, SAVE Leg 6	25°W	March 1989	SIO† (1992)

The historical data from *Meteor* 1925–1927 and from International Geophysical Year data are bottle data, whereas all other data sets are based on CTD measurements.

*SAVE Legs 1–3, Physical, chemical and CTD data, SIO Reference 92-9, unpublished report, 729 pp., Scripps Institution of Oceanography, University of California, San Diego, 1992.

†SAVE Leg 6, Physical, chemical and CTD data, SIO Reference 92-12, unpublished report, 190 pp., Scripps Institution of Oceanography, University of California, San Diego, 1992.

mass layer and the total transport in the box provided by the zonal section at 19°S (A9) and 30°S (A10) and the South American and African coastal boundaries were calculated with varying locations of the transition in levels of no motion. Minimizing the net mass balance in the box for each layer as well as the total box transport lead to the selection of transition locations indicated in Figure 6. The resulting water mass transports are listed in Table 3. Errors can mainly result from measurement noise, nonsynopticity of sections, insufficient spatial resolution, uncertainty in bottom topography, inappropriate bottom triangle approximations, and choices of levels of no motion. We have not attempted to quantify all these effects, because of a certain unavoidable arbitrariness in the criteria for levels of no motion. Considering results from similar studies and the check on bottom triangle contributions and on mass balance, a total transport error not exceeding 10–15% can probably be expected.

4. Deep Transports in the Southern Brazil Basin

The WOCE sections at 19°S and 30°S are now used to determine cumulative geostrophic transports across the entire South Atlantic of NADW and AABW. The results are presented in Figure 7. The Southern Brazil Basin between the Brazilian shelf and the Mid-Atlantic Ridge gains about 22 Sv of NADW through the northern section at 19°S (Figure 7a). We recognize two main branches of poleward flow, one with about 10 Sv close to the continental slope and a second one with about 12 Sv approximately 800 km off the shelf. At 30°S we find a poleward NADW flow of 10 Sv in the slope region (Figure 7b). Water mass properties indicate that this flow is the continuation of the branch of NADW found at 19°S close to the slope. A large part of NADW recirculates, however [see *Reid et al.*, 1977; *Zemba*, 1991; *Peterson*, 1992], and two northward flow cores occur just to the west and to the east of the Rio Grande Rise (Figure 7b). These cores can also be identified by high salinity values in water mass properties (Figure 5b). Owing to the recirculation the total poleward NADW transport between shelf and Mid-Atlantic Ridge at 30°S amounts to 6 Sv only. The total gain of NADW at the northern zonal sections is thus not balanced by an equal loss at the southern section, requiring an eastward export of NADW of 16 Sv across the Mid-Atlantic Ridge to the east. We note that the results from these new zonal sections lead to a pattern which is quite different from that in *Reid*'s [1989, Figure 24] map of adjusted steric height at 3000 dbar.

De Madron and Weatherly [1994] used SAVE sections at 18°S, 25°S, and 25°W and chose the same isopycnal surfaces bounding the NADW as listed in Table 2. They selected levels of no motion at the NADW/AABW interface whenever AABW was present and selected the AAIW/NADW interface otherwise. They found structures at their zonal sections at 18°S and 25°S which are similar to our results at 19°S and 30°S: two branches of southward NADW flow at the northern section and also a northward recirculation at the southern section. In the box given by the above sections, they obtained a gain of 12 Sv in the north and a gain of 1 Sv in the south which is not balanced by their eastward transport of 3–4 Sv. We suspect that this violation of continuity points to an inappropriate choice of reference levels in the central and eastern parts of the basin, as explained in our earlier discussion on the selection of levels of no motion.

In order to obtain more detailed information on the transport pattern in our region of study, we calculate the corresponding cumulative transports for the additional sections indicated in the map in Figure 8. For easier comparison the western part of the zonal WOCE section A9 at 19°S is repeated as section A. In the south, section D is in a similar position as the earlier presented WOCE section A10 at 30°S.

The western core in section A (about 10 Sv) can be found again in section C and in the western part of section D. Section B is influenced by the semistationary Vitória eddy described by *Brügge* [1992] and *Schmid et al.* [1995]. The overall balance again requires an eastward transport out of this area of more than 10 Sv. The results from our analysis are summarized in Figure 9. We note that *Fu* [1981] obtained an eastward NADW transport of about 16 Sv near 20°S from his inverse model. However, he did not resolve the western boundary transport farther south.

5. Changes of Potential Vorticity and the NADW Distribution

The concept of conservation of potential vorticity [see *Pedlosky*, 1979] provides a tool for understanding the observed

Table 2. Density Ranges of the Water Masses in the Southern Brazil Basin

	Upper Density Surface, kg m^{-3}	Lower Density Surface, kg m^{-3}
SF	ocean surface	$\sigma_0 = 27.10$
AAIW	$\sigma_0 = 27.10$	$\sigma_0 = 27.35$
UCPDW	$\sigma_0 = 27.35$	$\sigma_2 = 36.70$
NADW	$\sigma_2 = 36.70$	$\sigma_4 = 45.87$
AABW	$\sigma_4 = 45.87$	ocean bottom

SF, Surface Water; AAIW, Antarctic Intermediate Water; UCPDW, Upper Circumpolar Deep Water; NADW, North Atlantic Deep Water; and AABW, Antarctic Bottom Water.

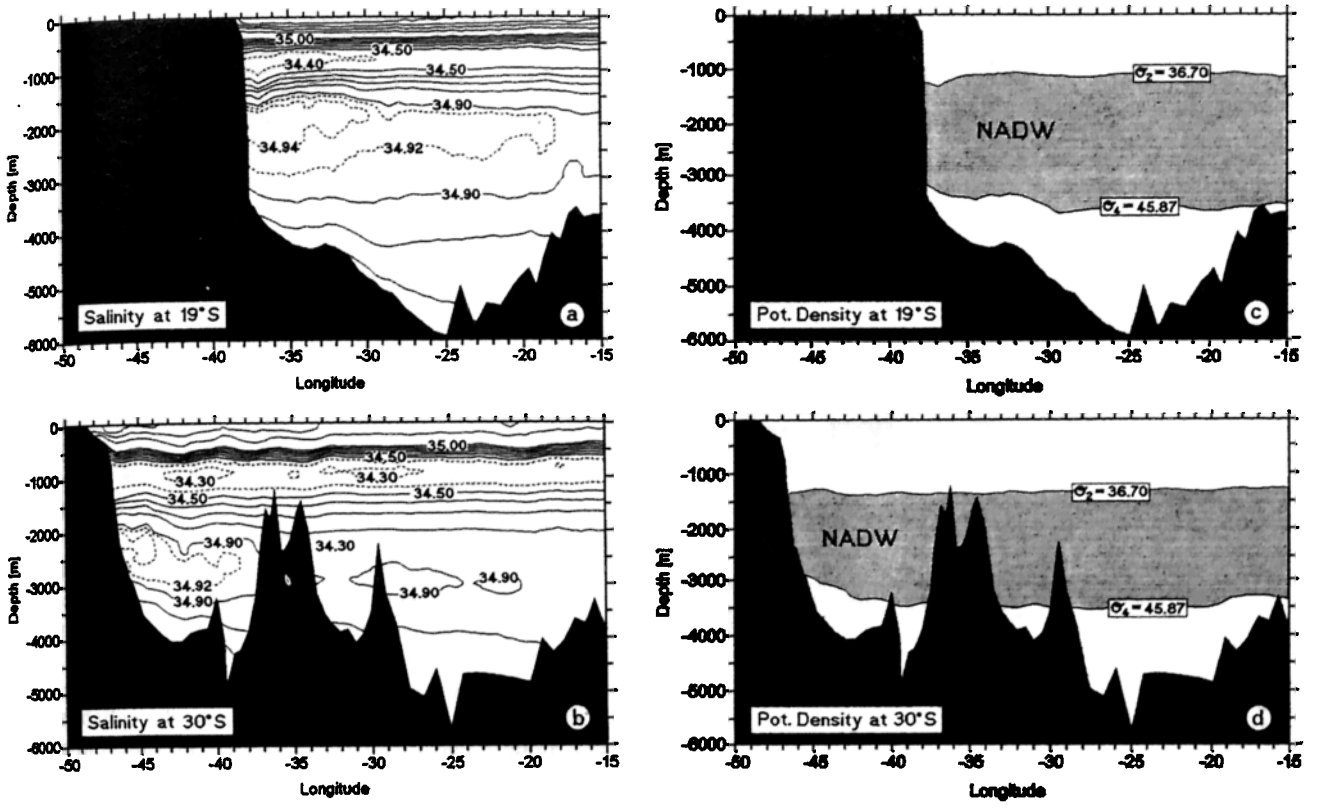

Figure 5. Vertical distribution of salinity (a) at 19°S and (b) at 30°S and depth of the upper and the lower density surface bounding the North Atlantic Deep Water (NADW) along (c) 19°S and (d) 30°S. Isohaline spacing below 500 m is $\Delta S = 0.1$. The cores of Antarctic Intermediate Water (AAIW) and NADW are marked by dashed isohalines at roughly 900 m and 2300 m.

NADW spreading in the western basin of the South Atlantic. The conservation of potential vorticity Q in large-scale flow is given by

$$\frac{dQ}{dt} = \frac{d}{dt}\left(\frac{f+\zeta}{H}\right) = 0 \Rightarrow Q = \frac{f+\zeta}{H} = \text{const}$$

with the Coriolis parameter $f = 2|\vec{\Omega}| \sin \varphi$ and the vertical component of the relative vorticity $\zeta = \vec{\zeta}_z$, while H is the vertical thickness of the water mass column. We assume that friction is negligible. In this case the water column will move along a trajectory which is controlled by its relative vorticity $\zeta = (\nabla \times \vec{u})_z$ and the geographic latitude φ only. If the water column is forced into zonal motion by a topographic obstacle, a change of ζ is required to balance the variation in H. In the southern hemisphere a water column will therefore rotate clockwise with increasing H. We suspect that the zonal Vitória-Trindade Ridge has a major effect on the spreading of NADW in the Southern Brazil Basin. To describe this influence, a simple conceptual model is developed. Its basic geometry is shown in Figure 10.

A wall from the bottom to the surface (depth $H_0 = 0$) represents the ridge and extends eastward from the western boundary through part of the box. The continental slope is represented by two steps, by areas with moderate depth H_1 just north and south of the wall, and by areas with larger depth H_2 farther east. The deep Brazil Basin is represented by the area

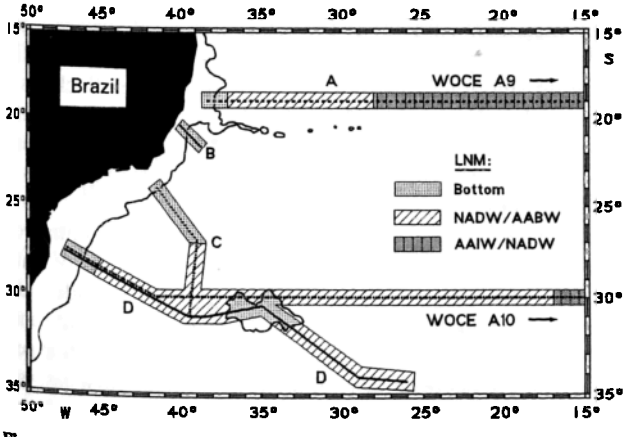

Figure 6. Levels of no motion (LNM) used for the geostrophic calculations presented in this study.

Table 3. Meridional Water Mass Transports in the Western and Eastern Basins of the South Atlantic

	Western Basin		Eastern Basin	
	19°S	30°S	19°S	30°S
SF	13.9	0.6	7.1	16.5
AAIW	2.7	0.8	1.0	3.1
NADW	−22.1	−6.3	−2.4	−16.5
AABW	5.6 (−4.2)	5.6	(−2.2)	(−3.5)

Values are given in sverdrups. Values in parentheses refer to transports in the density range defined as AABW here which are affected by some contribution from NADW.

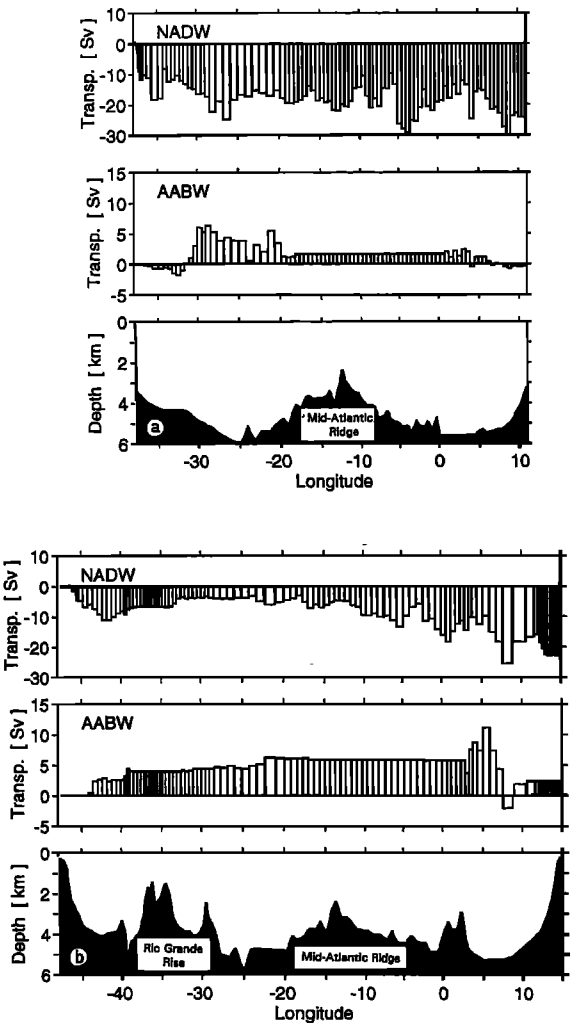

Figure 7. Cumulative geostrophic NADW and Antarctic Bottom Water (AABW) volume transports (a) along the zonal World Ocean Circulation Experiment (WOCE) section A9 at 19°S and (b) along WOCE section A10 at 30°S. Integration starts from the South American continent in the west, and positive values are to the north.

in the eastern part of the box, with depth H_3 slowly and linearly increasing from west to east. We assume that the density in the basin is constant and that the flow is inviscid.

It is assumed that water flowing southward along the western boundary is forced by the zonal ridge into an eastward direction. We then have an eastward flow with velocity u in the areas with H_1 and H_2 just north of the ridge. We consider a water column A at latitude φ_1 in the area with H_1 and another column B at latitude φ_2 in the area with H_2. Their potential vorticities are

$$Q_A = f(\varphi_1)/H_1 = \text{const}$$

$$Q_B = f(\varphi_2)/H_2 = \text{const}$$

respectively. At the line $x = x_0$ (see Figure 11) the water depth changes from H_1 to H_2. In order to preserve potential vorticity, column A has to gain negative relative vorticity ζ_A at this line.

$$f(\varphi_1)/H_1 = (f(\varphi_1) + \zeta_A(x_0))/H_2$$

or

$$\zeta_A(x_0) = f(\varphi_1)\left(\frac{H_2}{H_1} - 1\right) < 0$$

Column A starts to rotate clockwise. Compensation for this additional vorticity can be obtained by moving the column southward to higher latitudes. The change will be completely neutralized at the latitude φ_{neutr} where

$$f(\varphi_{\text{neutr}}) = f(\varphi_1) + \zeta_A(x_0)$$

or

$$\varphi_{\text{neutr}} = \arcsin\left(\frac{H_2}{H_1}\sin\varphi_1\right)$$

With frictional shear at the boundary we would have another clockwise component of relative vorticity which must be compensated by a southward movement.

Column B at initial depth H_2 does not experience the depth change at $x = x_0$, and potential vorticity is preserved if the column continues its zonal motion until $x = x_1$. There the depth begins to increase slowly, and the column will start to have a poleward component in its motion. Since the water parcel has time to adjust because of the slow change, it will move along a line with $f/H_3 = \text{const}$. The different paths of columns A and B are indicated in Figure 10.

Up to this point we have assumed a homogeneous ocean and a motion of a water column bounded by surface and bottom. We now modify the model considering the NADW as a decoupled layer. The isopycnal surface $\sigma_2 = 36.7\ \text{kg m}^{-3}$, that is, the transition from AAIW to NADW, is chosen as the layer's upper boundary, and the isopycnal surface $\sigma_4 = 45.87\ \text{kg m}^{-3}$, that is, the transition from NADW to AABW, is chosen as its lower boundary. No vertical transports exist through the upper and lower boundaries of the water mass column. Y. You and G. Siedler (personal communication, 1998) showed that in the region near 20°S in the western South Atlantic transports across neutral surfaces above and below the NADW core are particularly low, confirming the appropriateness of this assumption for this limited region near the western boundary. The vertical transports out of the NADW layer can thus be neglected, contrary to the vertical transports required in a Stommel-Arons model on the larger scales. Salt and heat are thereby also conserved within the layer.

To determine the local depths of the upper and lower boundaries, we use the complete oberservational database as summarized in Table 1. If the lower isopycnal surface is not observed at a certain location, we take the bottom instead. The resulting smoothed distribution of NADW layer thickness is presented in Figure 11. The layer thickness H_1 at the continental slope varies between 1300 and 1500 m. In the deep basin the thickness H_3 is typically 2000 m, with local variations of about ±200 m.

In Figure 12 we present contours of constant potential vorticity in the range corresponding to the transition of water column A from H_1 to H_2 north of the Vitória-Trindade Ridge at 19°S. The pattern indicates a flow along the continental slope to the south. The critical latitude φ_{neutr} is reached near 28°S, with the deepside part of the flow turning into a eastward direction. The corresponding model contours shown in Figure 13 indicate a predominantly zonal flow north of the ridge, with a moderate poleward turning of the deepside part of the flow

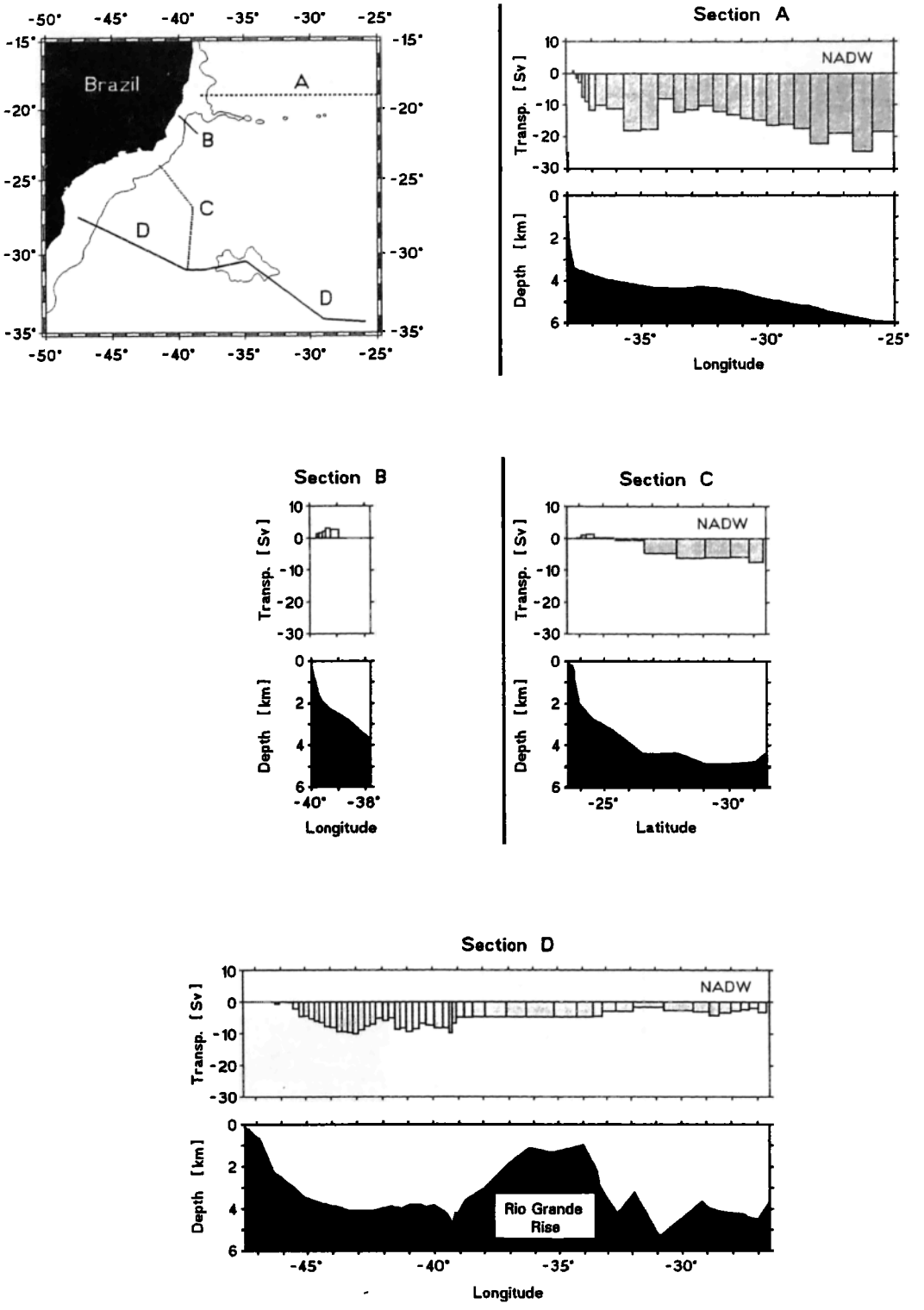

Figure 8. Cumulative geostrophic NADW transports along hydrographic sections A–D sampled during *Meteor* cruise 15 (December 30, 1990 to February 28, 1991). Integration starts from the South American continent in the west, and positive values are to the north. The bottom topography is shown in the map in the upper left corner with the 2000-m isobath indicated.

in the deep basin. The basic features of the potential vorticity pattern from our crude model appear to resemble the flow field derived from the observations of two branches in the region of study: a boundary transport along the continental slope and a predominantly eastward transport in the interior of the Southern Brazil Basin.

6. Conclusions

The North Atlantic Deep Water has three main branches in the South Atlantic. The present study was aimed at describing and explaining the branching which occurs at subtropical latitudes in the Brazil Basin. Using water mass criteria, some

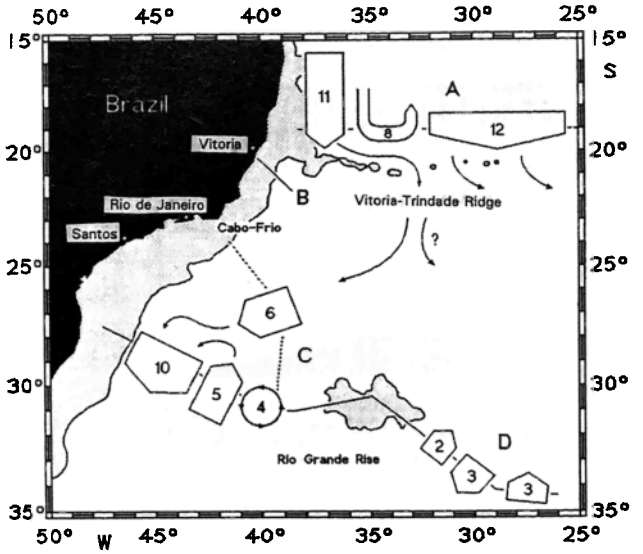

Figure 9. Schematic horizontal NADW transport pattern according to the data from *Meteor* cruise 15. Values are rounded to full sverdrups, and water depths less than 2000 m are shaded.

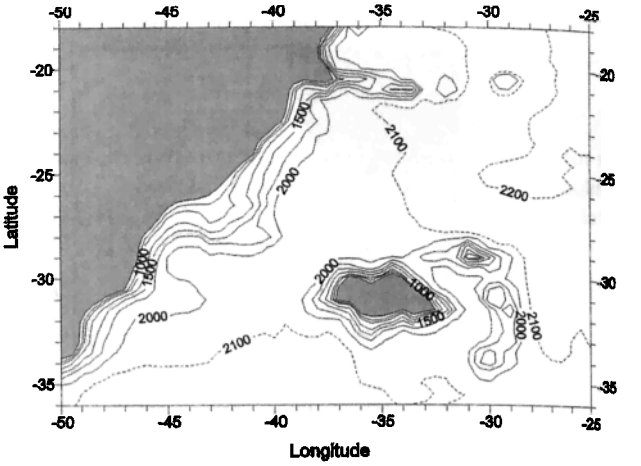

Figure 11. NADW layer thickness (in meters) interpolated from the observational data.

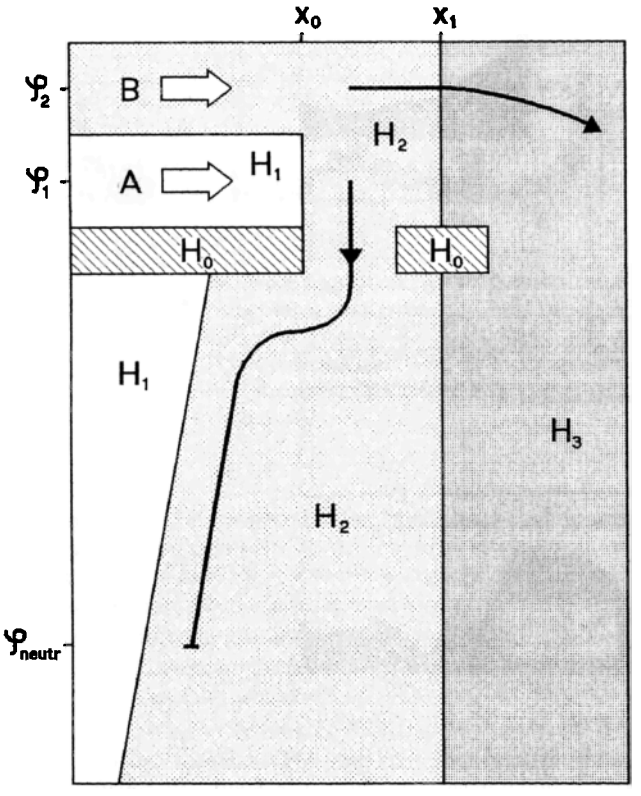

Figure 10. Presentation of the effects of changing water depth on a homogeneous water flow inhibited by a zonal ridge with depth $H_0 = 0$. The trajectories of two water columns A and B with constant potential vorticity Q are shown by lines with arrows. Southern hemisphere conditions are assumed ($f < 0$). The water depths are given by H_1 = const, $H_1 < H_2$ = const, and $H_2 < H_3$ which increases linearly to the east. The depth change of column A at x_0 is abrupt, while column B experiences a smooth transition at x_1 with the linear increase of depth.

fundamental knowledge about large-scale water mass spreading, and a mass balance constraint, we obtained levels of no motion with transitions from the lower NADW boundary to the upper NADW boundary in certain regions. With the absolute geostrophic flow field resulting from these levels, the transport pattern of NADW between 19°S and 30°S was determined for the western basin.

The region gains about 22 Sv of NADW at the northern boundary. Two branches with about 10 Sv and 12 Sv separate at the Vitória-Trindade Ridge near 20°S, with one southward branch along the continental slope and a second one with an easterly component. At the southern boundary a recirculation pattern exists, leading to a net southward transport of only 6 Sv. In order to close the balance, a major eastward transport out of the western basin and across the Mid-Atlantic Ridge between the above latitudes of about 16 Sv is required.

The simplified theoretical picture of the Stommel-Arons

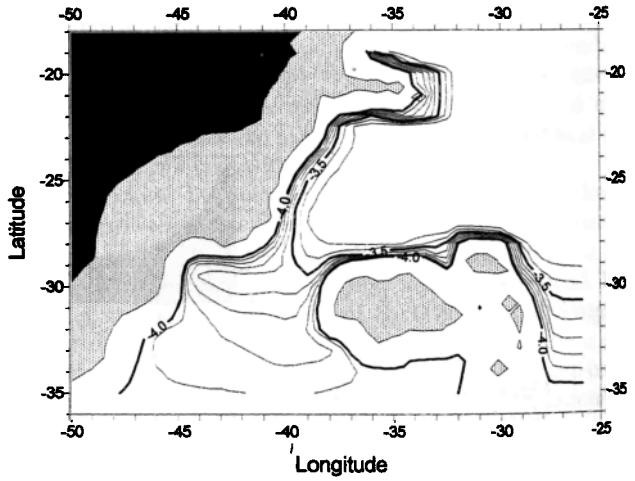

Figure 12. Contours of constant potential vorticity Q (in $10^{-8}\,m^{-1}\,s^{-1}$) corresponding to trajectories of water column A which is stretched from H_1 to H_2 in the model region north of the ridge at 19°S. H_2 is set at a fixed value of 2000 m, whereas H_1 varies for the different contour lines from 1250 m to 1500 m. Stipled areas represent regions where the model depth is less than 1500 m (corresponding to a real ocean depth $z <$ 3000 m).

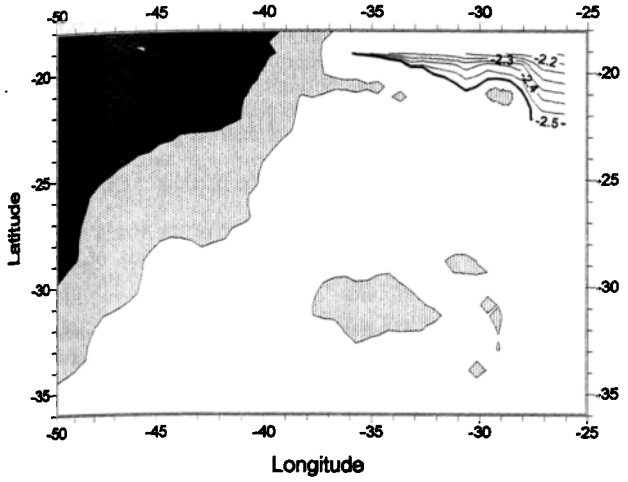

Figure 13. Contours of constant potential vorticity Q (in $10^{-8}\,m^{-1}\,s^{-1}$) corresponding to trajectories of water column B which has the initial depth H_2 in the model region north of the ridge at 19°S. H_2 varies between 2000 m and 2200 m. Stipled areas represent regions where the model depth is less than 1500 m (corresponding to a real ocean depth $z < 3000$ m).

model cannot be expected to explain such spatial patterns in the case of real bottom topography. By assuming that vertical transports through the upper and lower boundaries of the NADW layer can be neglected in the limited region near the western boundary, we can show that topographic control near the Vitória-Trindade-Ridge is responsible for the occurrence of branching. A simple model with varying depths is used to demonstrate that preservation of potential vorticity results in the branching in this area. It can also be shown that a large part of the along-slope southward flow turns into a zonal flow to the east at the latitudes where the change in planetary vorticity is sufficiently large to compensate for the change in potential vorticity due to the initial depth changes.

Acknowledgments. The authors want to express their thanks to the captains and crews of the research vessel *Meteor* and to the staff of the Marine Physics Department of the Institut für Meereskunde at Kiel University for their excellent assistance in obtaining and in processing the data sets. They appreciated the advice on text changes by an anonymous reviewer. The work was funded by the Ministry of Science and Technology (BMBF, WOCE II–IV) and by the German Research Foundation (DFG), Bonn, Germany. This is a WOCE contribution.

References

Boebel, O., C. Schmid, and W. Zenk, Flow and recirculation of Antarctic Intermediate Water across the Rio Grande Rise, *J. Geophys. Res.*, *102*, 20,967–20,986, 1997.

Brennecke, W., Ozeanographische Arbeiten der Deutschen Antarktischen Expedition (Pernambuco—Buenos Aires), III, Bericht, *Ann. Hydrogr. Mar. Meteorol.*, *39*, 642–647, 1911.

Broecker, W. S., The great ocean conveyer, *Oceanogr.*, *4*(2), 79–89, 1991.

Broecker, W. S., T. Takahashi, and Y.-H. Li, Hydrography of the central Atlantic, I, The two-degree discontinuity, *Deep Sea Res. Oceanogr. Abstr.*, *23*, 1083–1104, 1976.

Brügge, B., Oberflächendrifter auf METEOR Reise Nr. 15, in *WOCE Südatlantik 1991, Reise Nr. 15, 30. Dezember 1990–23. März 1991*, edited by G. Siedler and W. Zenk, *METEOR-Ber.*, *92-1*, pp. 52–55, Univ. Hamburg, Hamburg, Germany, 1992.

De Madron, X. D., and G. Weatherly, Circulation, transport and bottom boundary layers in the Brazil Basin, *J. Mar. Res.*, *52*, 583–638, 1994.

Friedrichs, M. A. M., M. S. McCartney, and M. M. Hall, Hemispheric asymmetry of deep water transport modes in the western Atlantic, *J. Geophys. Res.*, *99*, 25,165–25,179, 1994.

Fu, L. L., The general circulation and meridional heat transport of the subtropical South Atlantic determined by inverse methods, *J. Phys. Oceanogr.*, *11*, 1171–1193, 1981.

Fuglister, F. C., *Atlantic Ocean Atlas of Temperature and Salinity Profiles and Data From the International Geophysical Year of 1957–1958*, *Woods Hole Oceanogr. Inst. Atlas Ser.*, vol. I, 209 pp., Woods Hole Oceanogr. Inst., Woods Hole, Mass., 1960.

Gordon, A. L., and C. L. Greengrove, Geostrophic circulation of the Brazil-Falkland convergence, *Deep Sea Res., Part A*, *33*, 573–585, 1986.

Gouretski, V., and K. Jancke, A consistent pre-WOCE data set for the South Atlantic: Station data and gridded fields, *WHP Spec. Anal. Cent. Tech. Rep. 1* (*WOCE Rep. 127/95*), 81 pp., Bundesamt für Seeschiffahrt und Hydrogr., Hamburg, Germany, 1995.

Hogg, N., P. Biscaye, W. Gardner, and W. J. Schmitz Jr., On the transport and modification of Antarctic Bottom Water in the Vema Channel, *J. Mar. Res.*, *40*, suppl., 231–263, 1982.

Houry, S., E. Dombrowsky, P. de Mey, and J.-F. Minster, Brunt-Väisälä frequency and Rossby radii in the South Atlantic, *J. Phys. Oceanogr.*, *17*, 1619–1626, 1987.

Kuo, H. H., and G. Veronis, The use of oxygen as a test for an abyssal circulation model, *Deep Sea Res. Oceanogr. Abstr.*, *20*, 871–888, 1973.

McCartney, M. S., Crossing of the equator by the deep western boundary current in the western Atlantic Ocean, *J. Phys. Oceanogr.*, *23*, 1953–1974, 1993.

McCartney, M. S., and R. A. Curry, Transequatorial flow of Antarctic Bottom Water in the Western Atlantic Ocean: Abyssal geostrophy at the equator, *J. Phys. Oceanogr.*, *23*, 1264–1276, 1993.

Müller, T. J., Y. Ikeda, N. Zangenberg, and L. V. Nonato, Direct measurements of Western Boundary Currents off Brazil between 20°S and 28°S, *J. Geophys. Res.*, this issue.

Ollitrault, M., Y. Auffret, N. Cortès, C. Hémon, P. Jégou, S. Le Reste, G. Loaëc, and J.-P. Rannou, The SAMBA Experiment. *Rep. Ocean 2*, 488 pp., Inst. Fr. de Rech. pour l'Exploit. de la Mer, Plouzane, France, 1995.

Pätzold, J., K. Heidland, W. Zenk, and G. Siedler, On the bathymetry of the Hunter Channel, in *The South Atlantic: Present and Past Circulation*, edited by G. Wefer et al., pp. 351–358, Springer-Verlag, New York, 1996.

Pedlosky, J., *Geophysical Fluid Dynamics*, 2nd ed., Springer-Verlag, New York, 1979.

Peterson, R. G., The boundary currents in the western Argentine Basin, *Deep Sea Res., Part A*, *39*, 623–644, 1992.

Peterson, R. G., and T. Whitworth, The subantarctic and polar fronts in relation to deep water masses through the southwestern Atlantic, *J. Geophys. Res.*, *94*, 10,817–10,838, 1989.

Reid, J. L., On the total geostrophic circulation in the South Atlantic Ocean: Flow patterns, tracers and transports, *Prog. Oceanogr.*, *23*, 149–244, 1989.

Reid, J. L., W. D. Nowlin Jr., and W. C. Patzert, On the characteristics and circulation of the southwestern Atlantic Ocean, *J. Phys. Oceanogr.*, *7*, 62–91, 1977.

Rhein, M., L. Stramma, and U. Send, The Atlantic Deep Western Boundary Current: Water masses and transports near the equator, *J. Geophys. Res.*, *100*, 2441–2457, 1995.

Rintoul, S. R., South Atlantic Interbasin Exchange, *J. Geophys. Res.*, *96*, 2675–2692, 1991.

Schmid, C., H. Schäfer, G. Podesta, and W. Zenk, The Vitória eddy and its relation to the Brazil Current, *J. Phys. Oceanogr.*, *25*, 2532–2546, 1995.

Siedler, G., and W. Zenk, WOCE Südatlantik 1991, Reise Nr. 15, 30. Dezember 1990–23. März 1991, *METEOR Ber.*, *92-1*, 126 pp., Univ. Hamburg, Hamburg, Germany, 1992.

Siedler, G., W. Balzer, T. J. Müller, R. Onken, M. Rhein, and W. Zenk, WOCE South Atlantic 1992, Cruise No. 22, 22. September 1992–31. January 1993, *METEOR Ber.*, *93-5*, 131 pp., Univ. Hamburg, Hamburg, Germany, 1993.

Siedler, G., T. J. Müller, R. Onken, M. Arhan, H. Mercier, B. A. King, and P. M. Saunders, The zonal WOCE sections in the South Atlantic, in *The South Atlantic: Present and Past Circulation*, edited by G. Wefer et al., pp. 83–104, Springer-Verlag, New York, 1996.

Speer, K. G., and W. Zenk, The flow of Antarctic Bottom Water into the Brazil Basin, *J. Phys. Oceanogr.*, *23*, 2667–2682, 1993.

Stommel, H., The abyssal circulation, *Deep Sea Res.*, *5*, 80–82, 1958.

Stommel, H., and A. B. Arons, On the abyssal circulation of the world ocean, II, An idealized model of the circulation pattern and amplitude in ocean basins, *Deep Sea Res.*, *6*, 217–233, 1960.

Stommel, H., A. B. Arons, and A. J. Faller, Some examples of stationary flow patterns in bounded basins, *Tellus*, *10*(2), 179–187, 1958.

Tsuchiya, M., L. D. Talley, and M. S. McCartney, Water-mass distributions in the western South Atlantic: A section from South Georgia Island (54S) northward across the equator, *J. Mar. Res.*, *52*, 55–81, 1994.

Warren, B. A., Deep circulation of the world ocean, in *Evolution of Physical Oceanography*, edited by B. A. Warren and C. Wunsch, pp. 6–41, MIT Press, Cambridge, Mass., 1981.

Warren, B. A., and K. G. Speer, Deep circulation in the eastern South Atlantic Ocean, *Deep Sea Res., Part A*, *38*, suppl., 281–322, 1991.

Wüst, G., Schichtung und Zirkulation des atlantischen Ozeans: Die Stratosphäre des Atlantischen Ozeans, *Wissenschaftliche Ergebnisse der Deutschen Atlantischen Expedition auf dem Forschungs- und Vermessungschiff METEOR 1925–1927*, Band VI, Teil 1, pp. 110–288, Walter de Gruyter, Hawthorne, N. Y., 1935. (English translation, edited by W. J. Emery, Amerind, New Delhi, 1978.), (Available from Natl. Tech. Inf. Serv., Springfield, Va.)

Wüst, G., and A. Defant, Atlas zur Schichtung und Zirkulation des Atlantischen Ozeans, in *Wissenschaftliche Ergebnisse der Deutschen Atlantischen Expedition auf dem Forschungs- und Vermessungschiff METEOR 1925–1927*, Band VI (Atlas), Beil. I-CIII, Walter de Gruyter, Hawthorne, N. Y., 1936.

Zemba, J. C., The structure and transport of the Brazil Current between 27° and 36° South, Ph.D. thesis, Mass. Inst. of Technol.–Woods Hole Oceanogr. Inst., Woods Hole, Mass., 1991.

G. Siedler and N. Zangenberg, Institut für Meereskunde an der Universität Kiel, Düsternbrooker Weg 20, 24105 Kiel, Germany. (e-mail: gsiedler@ifm.uni-kiel.de)

(Received March 3, 1997; revised August 20, 1997;
accepted September 15, 1997.)